Post-ischaemic silencing of p66Shc reduces ischaemia/reperfusion brain injury and its expression correlates to clinical outcome in stroke

Spescha, R D ; Klohs, J ; Semerano, A ; Giacalone, G ; Derungs, R S ; Reiner, M F ; Rodriguez Gutierrez, D ; Mendez-Carmona, N ; Glanzmann, M ; Savarese, G ; Kränkel, N ; Akhmedov, A ; Keller, S ; Mocharla, P ; Kaufmann, M R ; Wenger, R H ; Vogel, J ; Kulic, L ; Nitsch, R M ; Beer, J H ; Peruzzotti-Jametti, L ; Sessa, Maria ; Lüscher, Thomas F ; Camici, G G

Abstract: Aim: Constitutive genetic deletion of the adaptor protein p66Shc was shown to protect from ischaemia/reperfusion injury. Here, we aimed at understanding the molecular mechanisms underlying this effect in stroke and studied p66Shc gene regulation in human ischaemic stroke. Methods and Results: Ischaemia/reperfusion brain injury was induced by performing a transient middle cerebral artery occlusion surgery on wild-type mice. After the ischaemic episode and upon reperfusion, small interfering RNA targeting p66Shc was injected intravenously. We observed that post-ischaemic p66Shc knockdown preserved blood-brain barrier integrity that resulted in improved stroke outcome, as identified by smaller lesion volumes, decreased neurological deficits, and increased survival. Experiments on primary human brain microvascular endothelial cells demonstrated that silencing of the adaptor protein p66Shc preserves claudin-5 protein levels during hypoxia/reoxygenation by reducing nicotinamide adenine dinucleotide phosphate oxidase activity and reactive oxygen species production. Further, we found that in peripheral blood monocytes of acute ischaemic stroke patients p66Shc gene expression is transiently increased and that this increase correlates with short-term neurological outcome. Conclusion: Post-ischaemic silencing of p66Shc upon reperfusion improves stroke outcome in mice while the expression of p66Shc gene correlates with short-term outcome in patients with ischaemic stroke.

DOI: https://doi.org/10.1093/eurheartj/ehv140

European Heart Journal Advance Access published April 22, 2015

European Heart Journal
doi:10.1093/eurheartj/ehv140

FASTTRACK BASIC SCIENCE

Post-ischaemic silencing of p66^{Shc} reduces ischaemia/reperfusion brain injury and its expression correlates to clinical outcome in stroke

R.D. Spescha[1,2], J. Klohs[3], A. Semerano[4], G. Giacalone[4], R.S. Derungs[5], M.F. Reiner[1,2], D. Rodriguez Gutierrez[1], N. Mendez-Carmona[1], M. Glanzmann[1,2], G. Savarese[1,2], N. Kränkel[1,2,6], A. Akhmedov[1,2], S. Keller[1,2], P. Mocharla[1,2], M.R. Kaufmann[2,7], R.H. Wenger[2,7], J. Vogel[8], L. Kulic[5], R.M. Nitsch[5], J.H. Beer[9], L. Peruzzotti-Jametti[4], M. Sessa[4], T.F. Lüscher[1,2,10], and G.G. Camici[1,2]*

[1]Center for Molecular Cardiology, University of Zurich, Wagistrasse 12, Schlieren CH-8952, Switzerland; [2]Zurich Center for Integrative Human Physiology (ZIHP), University of Zurich, Zurich, Switzerland; [3]Institute for Biomedical Engineering, Swiss Federal Institute of Technology Zurich (ETHZ), Zurich, Switzerland; [4]Department of Neurology, San Raffaele Scientific Institute, Milan, Italy; [5]Division of Psychiatry Research, University of Zurich, Schlieren, Switzerland; [6]Department of Cardiology, Charité - Universitätsmedizin Berlin, Campus Benjamin Franklin, Berlin, Germany; [7]Institute of Physiology, University of Zurich, Zurich, Switzerland; [8]Institute of Veterinary Physiology, University of Zurich, Zurich, Switzerland; [9]Department of Internal Medicine, Cantonal Hospital of Baden, Baden, Switzerland; and [10]Cardiology, University Heart Center, University Hospital, Zurich, Switzerland

Received 16 February 2015; revised 31 March 2015; accepted 6 April 2015

Aim Constitutive genetic deletion of the adaptor protein p66^{Shc} was shown to protect from ischaemia/reperfusion injury. Here, we aimed at understanding the molecular mechanisms underlying this effect in stroke and studied p66^{Shc} gene regulation in human ischaemic stroke.

Methods and results Ischaemia/reperfusion brain injury was induced by performing a transient middle cerebral artery occlusion surgery on wild-type mice. After the ischaemic episode and upon reperfusion, small interfering RNA targeting p66^{Shc} was injected intravenously. We observed that post-ischaemic p66^{Shc} knockdown preserved blood–brain barrier integrity that resulted in improved stroke outcome, as identified by smaller lesion volumes, decreased neurological deficits, and increased survival. Experiments on primary human brain microvascular endothelial cells demonstrated that silencing of the adaptor protein p66^{Shc} preserves claudin-5 protein levels during hypoxia/reoxygenation by reducing nicotinamide adenine dinucleotide phosphate oxidase activity and reactive oxygen species production. Further, we found that in peripheral blood monocytes of acute ischaemic stroke patients p66^{Shc} gene expression is transiently increased and that this increase correlates with short-term neurological outcome.

Conclusion Post-ischaemic silencing of p66^{Shc} upon reperfusion improves stroke outcome in mice while the expression of p66^{Shc} gene correlates with short-term outcome in patients with ischaemic stroke.

Keywords Stroke • Ischaemia • Reperfusion • Free radicals • Endothelium

Translational perspective

In light of the limited repertoire of therapeutical options available for the treatment of ischaemic stroke, the identification of novel potential targets is vital; in this respect, the present study demonstrates that the adaptor protein p66^{Shc} holds this potential as an adjunct therapy to thrombolysis. Post-ischaemic silencing of p66^{Shc} protein yielded beneficial effects in a mouse model of I/R brain injury underlying an interesting translational perspective for this target protein. Further, in proof-of-principle clinical experiments using PBMs, we demonstrate that p66^{Shc}

* Corresponding author. Tel: +41 44 635 64 68, Fax: +41 44 635 68 27, Email: giovanni.camici@uzh.ch; giovannicamici@hotmail.com

gene expression is transiently increased and that its levels correlate to short-term outcome in ischaemic stroke patients. Although these latter experiments are not directly relevant to the experiments performed in mice and in human endothelial cells, they provide novel important information about p66^{Shc} regulation in stroke patients and set the basis for further investigations aimed at assessing the potential for p66^{Shc} to become a novel therapeutic target as an adjunct of thrombolysis for the management of acute ischaemic stroke.

Introduction

Stroke is associated with major disabilities and mortality.[1] Although over the last decades several novel experimental neuroprotective strategies have been developed,[2] their translation into clinical practice has proven difficult.[3,4] Thus, the search for novel therapeutic targets for ischaemic stroke as an adjunct to thrombolysis remains an unmet clinical need.

Although ischaemic stroke is amenable to thrombolysis in patients presenting early after symptom onset,[5] vascular leakage and the ensuing oedema formation during reperfusion contributes importantly to neurological deficits.[6] Cerebral microvascular endothelial cells are a main component of the blood–brain barrier (BBB)[7] which divides the cerebral circulation from brain tissue. These cells are interconnected by tight and adherens junction proteins[7] whose integrity is critical for stroke outcome.[8] Indeed, disruption of the BBB following ischaemia/reperfusion (I/R) leads to vascular leakage and infiltration of plasma components into the brain tissue leading to oedema and further organ damage.[9–11] Overproduction of reactive oxygen species (ROS) following I/R is considered a key mechanism leading to BBB damage.[12] p66^{Shc}, an isoform of the mammalian adaptor protein Shc,[13,14] is a crucial mediator of ROS production in several disease states[15–18] thereby leading to cellular apoptosis.[19–21] Indeed, much of the vasculoprotective properties observed by genetic deletion of p66^{Shc} in mice are the result of reduced oxidative stress and in turn preserved endothelial function.[15–17]

In line with the above, we previously demonstrated that mice lacking p66^{Shc} develop smaller stroke size following I/R.[22] However, the clinical relevance of this observation remains unknown and the underlying molecular mechanisms poorly understood. To this end, we subjected mice to I/R brain injury and, to mimic real life clinical conditions as it would occur in the context of thrombolysis, we performed p66^{Shc} silencing *in vivo* using small interfering RNA (siRNA) after the ischaemic episode and upon reperfusion. Additionally, we mimicked I/R conditions in primary human brain microvascular endothelial cells (HBMECs) by exposing them to hypoxia/reoxygenation (H/R) with and without silencing of p66^{Shc} and assessed the production of ROS as well as the levels of tight and adherens junction proteins. Finally, we studied p66^{Shc} gene expression in peripheral blood monocytes (PBMs) of patients with acute ischaemic stroke and correlated it to the National Institutes of Health Stroke Scale (NIHSS).

Methods

Patients

Twenty-seven patients admitted to the emergency room of San Raffaele Hospital (OSR, Milan, Italy) with a diagnosis of acute ischaemic stroke presenting within 6 h from symptom onset were enrolled. Five patients presented wake-up stroke and were recruited within 6 h from awakening. The initial diagnosis was based on clinical history, neurological examination (conducted by certified neurologists), and a brain computed tomography (CT) scan. Nineteen sex- and age-matched healthy volunteers (either relatives or visitors of in-hospital patients), with a negative history of cardio- and cerebrovascular diseases, were included as controls. Patients diagnosed with diabetes, systemic inflammatory diseases, acute infections, and malignancy were excluded, to eliminate potential interference of those disease states on p66^{Shc} expression.[23] Blood was withdrawn from the antecubital vein at 6 and 24 h after initial stroke symptoms (for stroke patients), whereas control subjects donated blood once.

Of the 27 ischaemic stroke patients, 14 received thrombolytic treatment within 4.5 h from initial stroke symptoms onset. Ischaemic strokes were clinically classified according to the Oxford Community Stroke Project classification (also known as the Bamford or OXFORD classification).[24] Stroke aetiology was classified according to the Trial of ORG 10172 in Acute Stroke Treatment criteria.[25] Moreover, stroke severity was assessed, using NIHSS on admission and at discharge. Furthermore, delta NIHSS was calculated as the difference between the NIHSS presented at discharge and the NIHSS presented at admission (delta NIHSS = NIHSS discharge − NIHSS admission); thereby, positive values indicate short-term neurologic worsening while negative values indicate neurological improvement.

The study was approved by the local Ethics Committee at San Raffaele Scientific Institute, Milan, Italy. All participants (or their representative relatives) signed a written informed consent to authorize the treatment of their biological and clinical data.

Isolation of peripheral blood monocytes

Peripheral blood monocytes from whole blood were isolated using anti-CD14-coated MicroBeads (Miltenyi Biotec) on a magnetic separator (Miltenyi Biotec), as previously described.[26]

Animals

All animal experiments were performed on male, 11–13-week-old wild-type (wt) (C57/BL6J) mice. Study design and experimental protocols were approved by the Cantonal Veterinary Office of the Canton of Zurich.

Middle cerebral artery occlusion

A transient middle cerebral artery (MCA) occlusion (MCAO) surgery was performed on wt mice to induce I/R brain injury, as described.[22] In brief, anaesthesia was induced with 3% isoflurane in oxygen-enriched air and mice were kept under 1.5% isoflurane anaesthesia during MCAO surgery. Body temperature was controlled by using a warm water heating pad. Incision site was infiltrated with 0.5% bupivacaine solution for pain relief. A 6-0 silicone-coated filament (Doccol Corporation) was advanced into the internal carotid artery (ICA) until the thread occluded the origin of the left MCA to induce unilateral MCAO. After 45 min (60 min for evaluation of long-term effect) of ischaemia, the thread was removed to allow reperfusion of the MCA. After wound care and before returning to their standard cage, mice were kept for 1.5 h in a temperature controlled cage. For sham operation, the filament was advanced into the ICA without occluding the MCA.

In vivo p66^{Shc} silencing

In vivo p66^{Shc} silencing was performed as described.[27] Briefly, 1.6 nmol of predesigned siRNA targeting p66^{Shc} was incubated with a mixture of 150 mmol/L NaCl solution-jetPEI® and injected intravenously into the tail vein of the wt mouse randomized. Scrambled siRNA was used as a negative control. Detailed methods are provided in Supplementary material online.

Magnetic resonance imaging

Lesion development was monitored after MCAO on a Bruker PharmaScan 47/16 (Bruker BioSpin GmbH) operating at 4.7 T. Anaesthesia was induced using 3% isoflurane (Abbott) in a 4 : 1 air–oxygen mixture. During MRI acquisition, mice were kept under isoflurane anaesthesia (1.5%). During the scan session, body temperature was monitored with a rectal temperature probe (MLT415, ADInstruments) and kept at 36 ± 0.55°C using a warm water circuit integrated into the animal support (Bruker BioSpin GmbH). Magnetic resonance imaging (MRI) recordings were done in a blinded way by an independent person.

The lesion was determined on maps of the apparent diffusion coefficient (ADC) derived from diffusion-weighted images as areas of significant reduction of the ADC compared with the unaffected, contralateral side. The lesion in the T2-weighted image was determined as hyperintense areas compared with the contralateral hemisphere. Lesion volumes were quantified blinded by drawing regions of interest around the areas of reduced ADC and hyperintensities in T2-weighted images in five MRI slices using an ROI tool (Paravision, Bruker). Brain infarct volumes were calculated by summing the volumes of each section and correcting for brain swelling, as described.[28] Detailed methods are provided in Supplementary material online.

Neurological deficits measurement

Neurological status was assessed using an adapted four-point scale test based on Bederson *et al.*[29] and was graded as previously described[22]: Grade 0: normal neurological function; Grade 1: forelimb flexion; Grade 2: circling; Grade 3: leaning to the contralateral side at rest; Grade 4: no spontaneous motor activity. Motor performance was assessed using the RotaRod test. Mice were placed on a rotating rod with increasing speed (4–44 revolutions/min; circumference of the rod: 9 cm) and the latency to fall was measured. The experimental trail was ended if the maximum rotation speed was achieved or if the mouse fell off the rod. Per time point, three test runs per mouse were performed and the best run was included in the statistics. Neurological deficit measurements were performed in a blinded way.

Evaluation of long-term effect

Long-term effect of post-ischaemic *in vivo* p66^{Shc} silencing on stroke was assessed up to 6 days. The well-being of mice during the experimental period was determined using a score sheet that was approved by the Cantonal Veterinary Office of the Canton of Zurich. This score sheet was used to define survival/death of an animal. Death events include spontaneous deaths (4 of 16 for siScr stroke mice and 3 of 15 for sip66^{Shc} stroke mice) and mice which did not fulfil the health evaluation criteria.

Evans blue extravasation

Determination of BBB permeability after MCAO was done by evaluating Evans blue extravasation, as described.[30] Detailed methods are provided in Supplementary material online.

Immunofluorescence staining

Frozen brains were cut into 6 μm thick slices on a cryostat (Leica Cm 1900). Immunofluorescent analysis was performed as described.[31] Briefly, brain slices were fixed in 4% paraformaldehyde and incubated with primary and secondary antibodies. Images were taken using a Leica Dm4000 B microscope. Stained area of claudin-5, vascular endothelial (VE)-cadherin, or occludin was measured using ImageJ Software and normalized to the total endothelial cell surface (assessed by isolectin B_4 staining). Detailed methods are provided in Supplementary material online.

RNA isolation and reverse transcription

Total RNA isolation and preparation of cDNA was performed as previously described.[26] Total RNA of PBM, or of MCA, was extracted using TRIzol Reagent (Invitrogen). Two micrograms (MCA) or 1 μg (PBM) of RNA was reverse transcribed using Ready-To-Go You-Prime First-Strand Beads (Amersham Biosciences) and first-strand random cDNA primers pd(N)6 (TaKaRa).

Real-time polymerase chain reaction

Determination of p66^{Shc} gene expression was done as previously described.[26] Detailed methods are provided in Supplementary material online.

Cell culture experiments

Primary HBMECs (Cell Systems) were cultured in EBM-2 medium supplied with EGM-2 bullet kit (Lonza). Adhering cells (passages 5–9) were grown to confluence and exposed to hypoxia (0.2% oxygen) for 4 h, followed or not by 4 h of incubation in a normoxic incubator (reoxygenation). Hypoxia was induced using a gas-controlled glove box (Invivo2 400, Ruskinn Technologies). In certain experiments, cells were pre-incubated with apocynin (0.1 mmol/L) (SAFC) for 1 h. Thereafter, HBMECs were harvested for measuring superoxide anion (O_2^-) production, nitric oxide (NO) bioavailability, nicotinamide adenine dinucleotide phosphate (NADPH) oxidase activity or immunoblot analysis.

Small interfering RNA transfection in human brain microvascular endothelial cells

Human brain microvascular endothelial cells were incubated with predesigned siRNA targeting p66^{Shc} at final concentration of 25 nmol/L using lipofectamine®RNAiMAX Reagent (Invitrogen), as previously described.[32] Detailed methods are provided in Supplementary material online.

Immunoblotting

Basilar arteries and cells were lysed in lysis buffer and proteins were separated using SDS–PAGE, as previously described.[32] Detailed methods are provided in Supplementary material online.

Measurement of O_2^- production and nitric oxide bioavailability

Electron spin resonance spectroscopy was applied to determine O_2^- production and NO bioavailability, as described.[27,32–34] Detailed methods are provided in Supplementary material online.

Nicotinamide adenine dinucleotide phosphate oxidase activity

Nicotinamide adenine dinucleotide phosphate oxidase activity was determined indirectly by measuring the ratio of NADP/NADPH using a commercially available kit (Abcam), according to the manufacturer's recommendations.

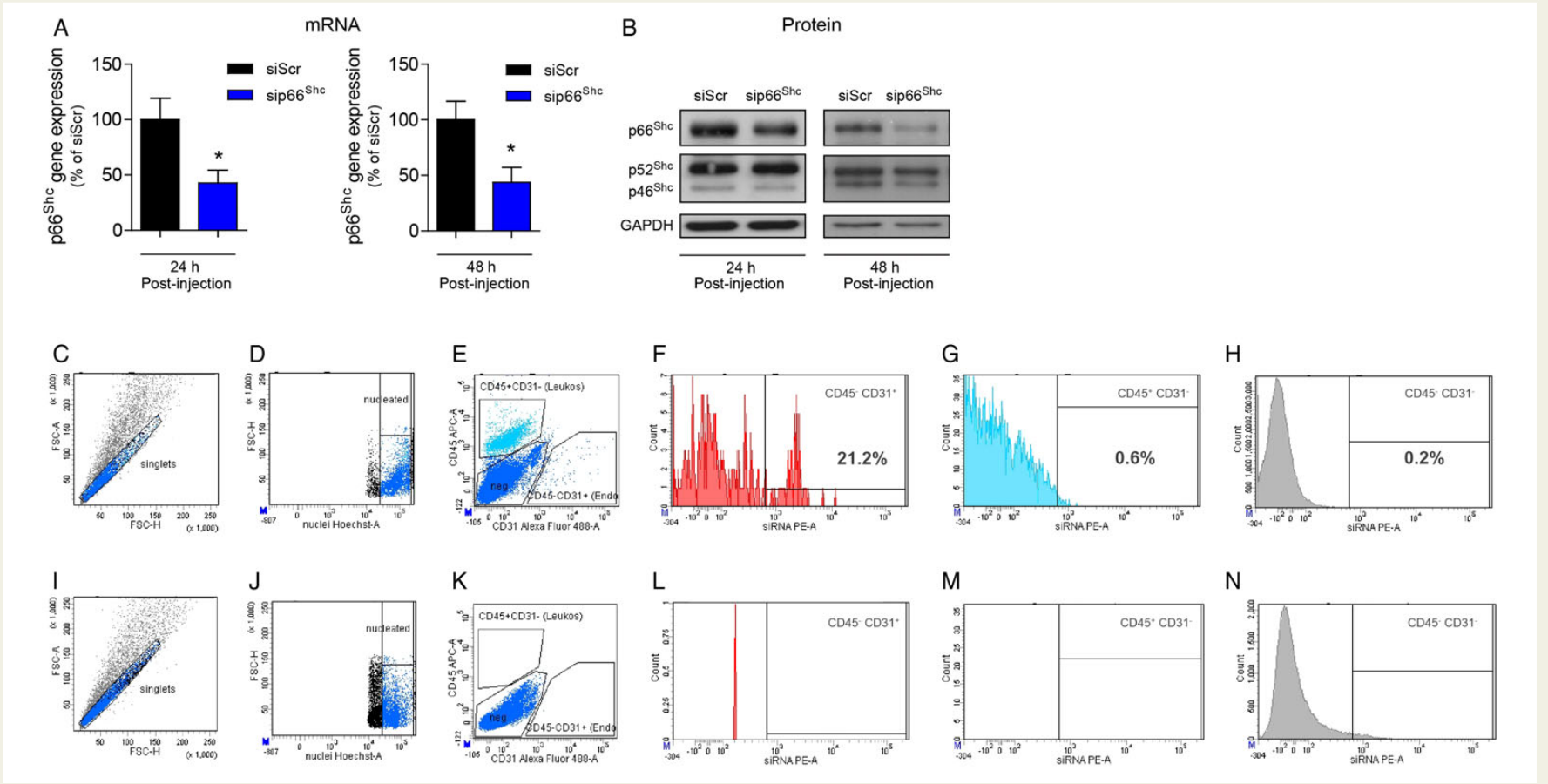

Figure 1 *In vivo* silencing of p66^{Shc}. (*A*) Real-time polymerase chain reaction reveals reduced p66^{Shc} levels in middle cerebral artery homogenates 24 h ($n = 5–6$) and 48 h ($n = 7–8$) after p66^{Shc} small interfering RNA injection compared with scrambled small interfering RNA injection (siScr). Data are expressed as mean ± s.e.m. *$P < 0.05$ for sip66^{Shc} vs. siScr. (*B*) Immunoblot analysis confirms silencing of p66^{Shc} in basilar arteries within 48 h after p66^{Shc} small interfering RNA injection (representative immunoblot of at least five animals per group). (*C–N*) Flow cytometry analysis of brain single cell suspensions 24 h after injection of Alexa546-sip66^{Shc} (upper panel) when compared with negative control (lower panel). Singlets (*C* and *I*) with nuclei (*D* and *J*) were plotted in a dot plot of APC (CD45) vs. AlexaFluor488 (CD31) to distinguish endothelial cells (CD45$^-$CD31$^+$), leukocytes (CD45$^+$CD31$^-$), as well as other cell types (CD45$^-$CD31$^-$) (*E* and *K*). Histogramms show Alexa546-fluorescence representing content of Alexa546-sip66^{Shc} in endothelial cells (*F* and *L*), leukocytes (*G* and *M*), and other cell types (*H* and *N*).

Statistical analysis

Statistical analysis for comparison of two groups was performed using two-tailed unpaired Student's *t*-test, or Mann–Whitney test, when appropriate. For comparison of more than two unmatched groups, one-way analysis of variance (ANOVA) followed by Bonferroni *post hoc* test, or Kruskal–Wallis test followed by Dunn's *post hoc* test, when appropriate, was performed. For comparison of groups with repeated measures, two-way ANOVA followed by Bonferroni *post hoc* test was applied. Statistical analysis for survival studies was performed using log-rank (Mantel-Cox) test. Pearson's correlation analysis was used to test the correlation between two quantitative variables, and Fisher's exact test for comparison of categorical data between study subjects. Two-sided *P*-values were calculated and $P < 0.05$ denoted a significant difference. Statistical analysis was performed using GraphPad Prism® software 5.01.

Results

In vivo post-ischaemic silencing of p66^{Shc} reduces lesion volumes and improves functional outcome following I/R brain injury

To study the effect of post-ischaemic p66^{Shc} silencing on stroke, a transient MCAO surgery was performed on wt mice to induce I/R brain injury. To analyse p66^{Shc} silencing efficiency *in vivo* beforehand, p66^{Shc} mRNA and protein levels were quantified in cerebral arteries (MCA and basilar artery, respectively). Intravenous injection of siRNA against p66^{Shc} reduced mRNA and protein p66^{Shc} levels within 48 h after injection compared with siScr injection (*Figure 1A* and *B*). To localize the distribution of the p66^{Shc} siRNA within brain cerebral arteries, wt mice were injected with fluorescence dye-labelled p66^{Shc} siRNA (Alexa546-sip66^{Shc}). Flow cytometry with whole brain digests revealed a predominant uptake of the siRNA by the brain endothelium. We observed that 21.2% of brain endothelial cells (CD45^{-}CD31^{+}) showed a positive signal for Alexa546-tagged p66^{Shc} siRNA (*Figure 1F*) while only 0.6% of leukocytes (CD45^{+}CD31^{-}) (*Figure 1G*) and 0.2% of other nucleated cells (CD45^{-}CD31^{-}) (*Figure 1H*) were positive for the Alexa546 signal. Negative control was stained with Hoechst 33342 to label nucleated cells (*Figure 1L–N*).

Lesion volumes in sip66^{Shc} and siScr injected stroke mice were quantified with MRI. Diffusion-weighted imaging (DWI) denoted matching baseline lesion sizes in both groups after 45 min of ischaemia and directly upon reperfusion (*Figure 2B*). At 48 h post-MCAO, both DWI and T2-weighted imaging displayed instead a reduced stroke volume in sip66^{Shc} stroke mice when compared with siScr stroke mice (*Figure 2B* and *C*).

Neurological deficits after MCAO were assessed using two different tests. Pre-MCAO, both sip66^{Shc} and siScr stroke mice showed

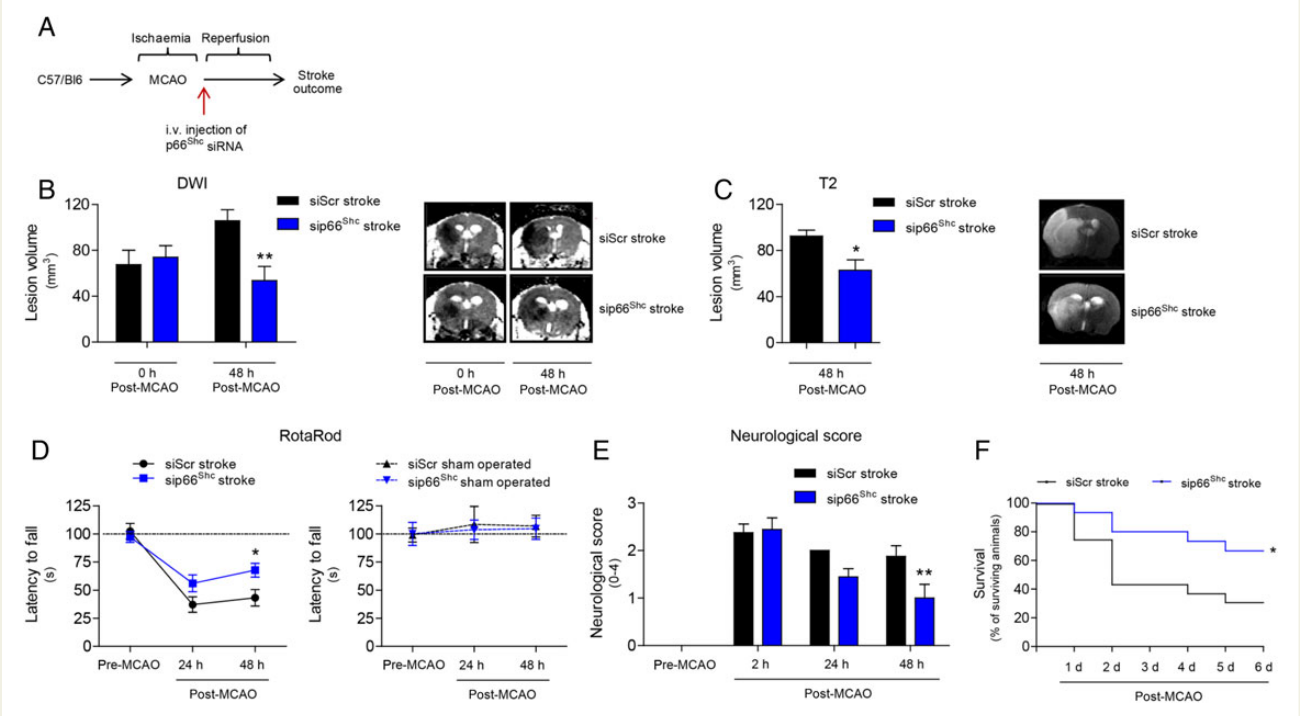

Figure 2 Impact of post-ischaemic *in vivo* p66^{Shc} silencing on stroke outcome. (*A*) Schematic of experimental study design. Upon reperfusion, specific small interfering RNA against p66^{Shc} is injected intravenously in wt mice, and development of lesion and functional deficits were characterized. (*B* and *C*) Both, DWI and T2-weighted imaging denote reduced lesions in sip66^{Shc} stroke mice (DWI: $n = 5$; T2: $n = 6$) compared with siScr stroke mice ($n = 7$) at 48 h post-MCAO. (*D* and *E*) Evaluation of neurological deficits by using the RotaRod test and a four-point scale test based on Bederson *et al.*[28] Both neurological tests demonstrate less neurological deficits in the sip66^{Shc} stroke group ($n = 9$) compared with the siScr stroke group (RotaRod: $n = 7$; Bederson: $n = 8$). All sham operated animals show normal neurological function throughout the experimental period ($n = 5–6$). (*F*) Post-ischaemic silencing of p66^{Shc} increases survival of mice after stroke ($n = 15–16$). Data are expressed as mean ± s.e.m. $^{*}P < 0.05$, $^{**}P < 0.01$ for sip66^{Shc} stroke vs. siScr stroke.

comparable performance in the RotaRod test and on the four-point scale test based on Bederson *et al.*[29] (*Figure 2D* and *E*). At 24 h post-MCAO, we observed in both groups a reduced latency to fall in the RotaRod test. However, at 48 h post-MCAO, sip66^{Shc} stroke mice showed a significant higher persistence on the rotating drum compared with siScr stroke mice (*Figure 2D*). In line with that, neurological deficits assessed with the scale test were significantly lower in sip66^{Shc} stroke mice compared with siScr stroke mice at 48 h post-MCAO (*Figure 2E*). All sham operated animas displayed normal neurological functions throughout the experimental period (*Figure 2D* and data not shown).

By analysing the impact of p66^{Shc} silencing on stroke up to 6 days, we found an improved survival of sip66^{Shc} stroke mice when compared with siScr stroke mice (*Figure 2F*, 31.25% survival for siScr stroke mice vs. 66.66% for sip66^{Shc} stroke mice). Survival was assessed in accordance to the health evaluation criteria approved by the Cantonal Veterinary Office of the Canton of Zurich; all sham operated animals survived and fulfilled the health evaluation criteria (data not shown).

In vivo p66^{Shc} silencing preserves blood–brain barrier integrity after I/R brain injury

The BBB plays a critical role for the outcome of stroke,[8] and its permeability can be assessed *in vivo* by quantifying Evans blue extravasation.[9,30] We tested whether post-ischaemic p66^{Shc} silencing preserves BBB permeability after I/R brain injury in mice. Indeed, 48 h post-MCAO p66^{Shc} silencing reduced Evans blue extravasation when compared with mice receiving siScr (*Figure 3A*).

Blood–brain barrier permeability is regulated by tight and adherens junctional proteins connecting cerebral microvascular endothelial cells.[35] Thus, we analysed the integrity of tight and adherens junctions following I/R brain injury focusing on claudin-5, occludin, and VE-cadherin. Immunofluorescence staining of claudin-5 on coronal brain sections of siScr-treated stroke mice revealed decreased claudin-5-positive stained areas normalized to the total endothelial surface (measured by isolectin B_4 staining[31,36]) in the ipsilateral hemisphere compared with the contralateral hemisphere (*Figure 3B*), while this disruption of claudin-5 integrity was not observed in stroke mice receiving sip66^{Shc} (*Figure 3B*). Unlike claudin-5, occludin and VE-cadherin-positive stained areas were not changed following I/R brain injury in both experimental groups (data not shown).

Role of p66^{Shc} in H/R in primary human brain microvascular endothelial cells

In order to characterize the molecular regulation of claudin-5 by p66^{Shc} and to translate our *in vivo* murine data to human cells, we exposed HBMECs to hypoxia (H) alone, or hypoxia followed by reoxygenation (H/R). Exposure of HBMECs to hypoxia neither altered phosphorylation of p66^{Shc} at Ser36, a critical step for its pro-apoptotic[37] and pro-oxidant activity,[21] nor total p66^{Shc} protein

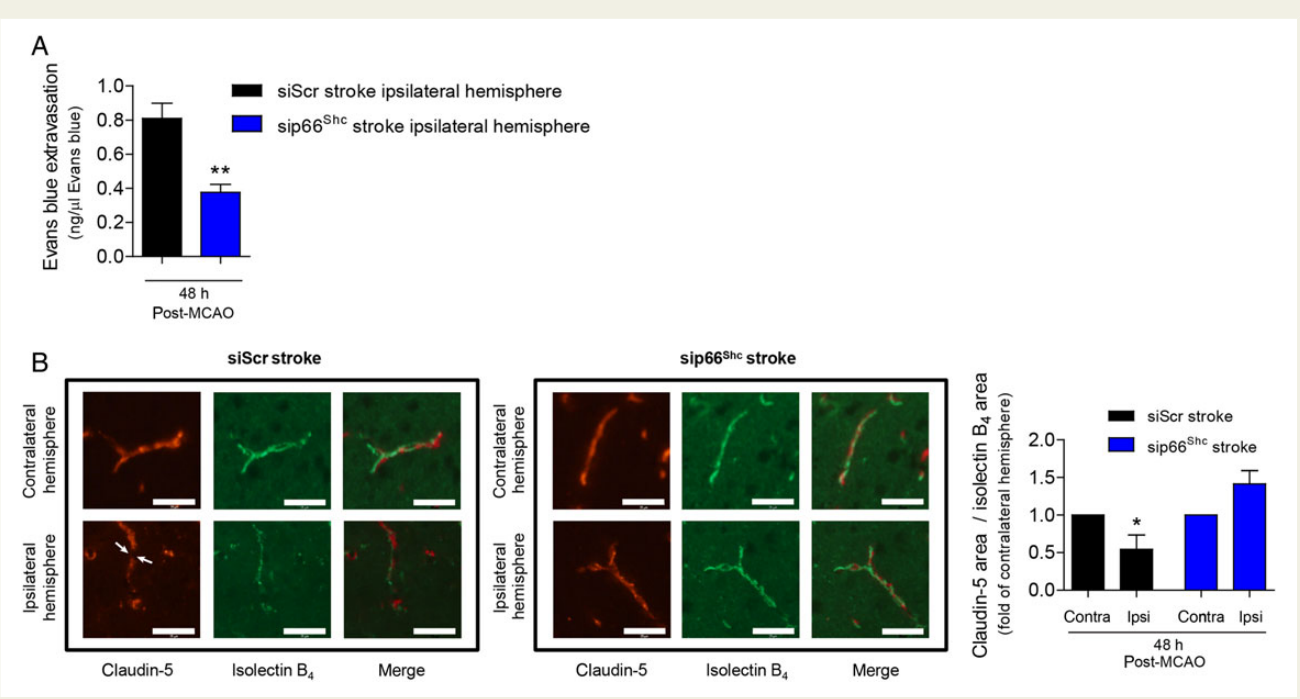

Figure 3 p66^{Shc} mediates blood–brain barrier disruption after I/R brain injury. (*A*) Assessment of blood–brain barrier impairment. p66^{Shc} silenced mice ($n = 6$) show less Evans blue extravasation compared with siScr stroke mice ($n = 5$) at 48 h of reperfusion. (*B*) Representative fluorescence microscopy images of claudin-5 and isolectin B_4 (endothelial marker) stained brain sections. Following I/R brain injury, claudin-5-positive stained area normalized to the total endothelial surface is reduced in the ipsilateral hemisphere compared with the contralateral hemisphere in siScr stroke mice ($n = 5$), but not in sip66^{Shc} stroke mice ($n = 5$). Scale bar, 35 µm. Data are presented as mean ± s.e.m. *$P < 0.05$ for siScr stroke ipsilateral vs. siScr stroke contralateral; **$P < 0.01$ for sip66^{Shc} stroke vs. siScr stroke.

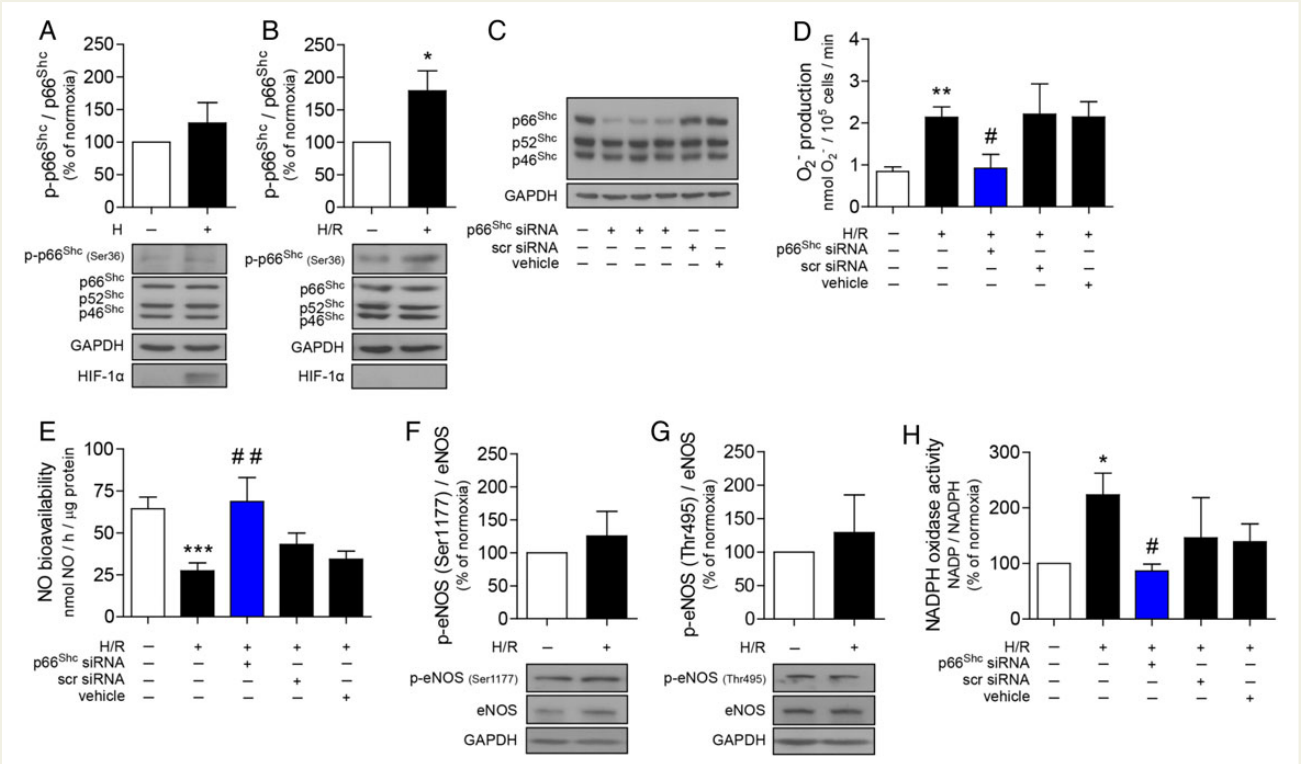

Figure 4 p66^{Shc} mediates H/R-induced damage of human brain microvascular endothelial cells. (*A*) p66^{Shc} activation remains unchanged after exposure of human brain microvascular endothelial cells to hypoxia compared with normoxia ($n = 8$). Hypoxia-inducible factor-1α stabilization is used as an indicator for effective hypoxic condition. (*B*) Hypoxia followed by reoxygenation increases phosphorylation of p66^{Shc} at Ser36 compared with normoxia ($n = 6$). (*C*) Representative immunoblot of p66^{Shc} silencing *in vitro*. Pre-incubation of human brain microvascular endothelial cells with p66^{Shc} small interfering RNA selectively reduces p66^{Shc} levels, without affecting the levels of the two other Shc isoforms p52^{Shc} and p46^{Shc}. (*D*) H/R leads to an increased O_2^- production ($n = 12–13$) that is blunted after silencing of p66^{Shc} ($n = 7–13$). (*E*) Human brain microvascular endothelial cells exposed to H/R show a reduced nitric oxide bioavailability ($n = 12$) that is elevated after p66^{Shc} silencing ($n = 6–12$). (*F* and *G*) H/R does not alter phosphorylation of endothelial NO synthase at both sites studied (Ser1177 and Thr495) and endothelial NO synthase protein expression compared with normoxia ($n = 7$). (*H*) Pre-incubation of human brain microvascular endothelial cells with p66^{Shc} small interfering RNA reduces H/R-increased nicotinamide adenine dinucleotide phosphate oxidase activity ($n = 11$). Data are expressed as mean ± s.e.m. $^*P < 0.05$, $^{**}P < 0.01$, $^{***}P < 0.001$ for H/R vs. normoxia; $^{\#}P < 0.05$, $^{\#\#}P < 0.01$ for H/R with sip66^{Shc} vs. H/R.

levels significantly, compared with normoxia (*Figure 4A*). In contrast, exposure to H/R increased phosphorylation of p66^{Shc} at Ser36 compared with normoxia (*Figure 4B*). Hypoxia-inducible factor-1α protein stabilization was used as an indicator of effective hypoxic conditions (*Figure 4A*). Reactive oxygen species and NO are critical for endothelial function[20] and have been implicated in vascular permeability.[12] Here, we analysed whether H/R regulates O_2^- production and NO bioavailability, and whether p66^{Shc} mediates these effects. Exposure of HBMECs to H/R led to an increased O_2^- production (*Figure 4D*) and a decreased NO bioavailability (*Figure 4E*) compared with normoxia. However, endothelial NO synthase (eNOS) phosphorylation at both sites studied (Ser1177 and Thr495) and eNOS protein expression remained unchanged (*Figure 4F* and *G*). Pre-incubation of HBMECs with p66^{Shc} siRNA, but not scrambled siRNA, reduced the increased O_2^- production (*Figure 4D*) and increased the reduced NO bioavailability during H/R (*Figure 4E*). Nicotinamide adenine dinucleotide phosphate oxidase is considered as a major source of vascular O_2^-,[38] and is a downstream target of p66^{Shc}.[34,39] Moreover, NADPH oxidase was demonstrated to play a dominant role in ROS production in brain endothelial cells exposed to H/R.[40] Thus, we investigated whether during H/R NADPH oxidase is a source of O_2^- production downstream of p66^{Shc}. Indeed, NADPH oxidase activity was increased after exposure to H/R, and returned to control levels after silencing of p66^{Shc} (*Figure 4H*).

Effect of p66^{Shc} and reactive oxygen species on claudin-5 *in vitro*

Human brain microvascular endothelial cells exposed to H/R exhibited reduced protein levels of claudin-5 compared with normoxia (*Figure 5A*). In contrast, occludin and VE-cadherin protein levels were not affected by exposure to H/R (*Figure 5B* and *C*). After both, pre-incubation of HBMECs with p66^{Shc} siRNA and with the antioxidant apocynin[41] claudin-5 levels were elevated under H/R condition (*Figure 5D* and *E*).

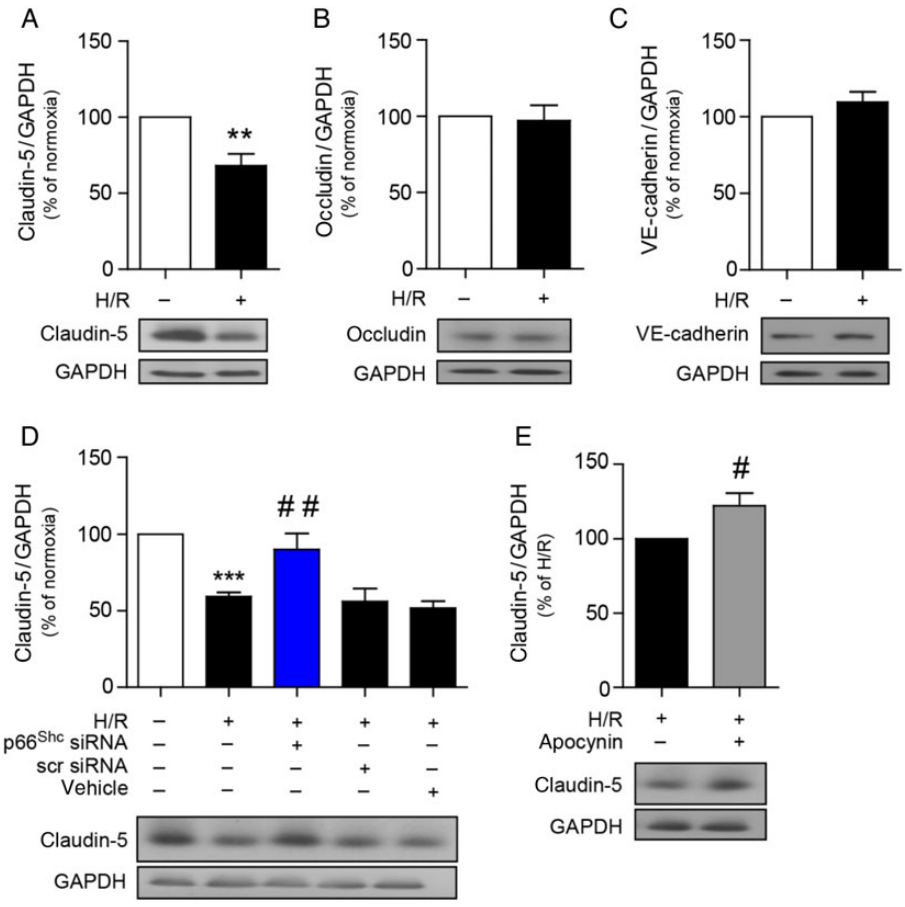

Figure 5 Effect of p66^{Shc} silencing and reactive oxygen species on H/R-decreased claudin-5 expression. (*A*) Immunoblot analysis reveals decreased claudin-5 protein levels after exposure of human brain microvascular endothelial cells to H/R ($n = 7$), but not of occludin ($n = 5$) (*B*) and vascular endothelial-cadherin ($n = 7$) (*C*). Pre-incubation with p66^{Shc} small interfering RNA ($n = 7$) (*D*), or apocynin (0.1 mmol/L) ($n = 6$) (*E*), increases claudin-5 levels under H/R condition. Data are presented as mean ± s.e.m. $^{**}P < 0.01$, $^{***}P < 0.001$ for H/R vs. normoxia; $^{\#}P < 0.05$, $^{\#\#}P < 0.01$ for H/R with sip66^{Shc} or apocynin vs. H/R.

p66^{Shc} gene expression is increased in patients with ischaemic stroke and correlates to neurological outcome

To provide evidence for a role of p66^{Shc} in human ischaemic stroke, we analysed p66^{Shc} expression in PBMs of patients with ischaemic stroke. A total of 27 ischaemic stroke patients and 19 age- and sex-matched, healthy control subjects were recruited. Clinical characteristics of both groups did not differ statistically (*Table 1*). p66^{Shc} mRNA levels were significantly increased 6 h after initial stroke symptoms (*Figure 6A*) and returned to control levels 24 h thereafter (*Figure 6A*). Of note, p66^{Shc} gene expression at 6 h was comparable in patients with ischaemic stroke regardless of whether they had received thrombolytic treatment or not (*Figure 6B*). p66^{Shc} transcript levels of all study subjects positively correlated with neurological deficits at admission, measured according to the NIHSS (*Figure 6C*). Importantly, while p66^{Shc} gene expression of stroke patients which did not receive thrombolytic intervention did not correlate with short-term neurological outcome (NIHSS discharge − NIHSS admission) (*Figure 6D*), it positively correlated in stroke patients treated with thrombolysis (*Figure 6E*).

Discussion

In this study, we demonstrate for the first time that post-ischaemic p66^{Shc} silencing reduces brain injury by preserving BBB integrity by preventing claudin-5 level downregulation. The *in vivo* findings in the mouse were translated to HBMECs exposed to H/R where p66^{Shc} was phosphorylated at Ser36 leading to the reduction in claudin-5 levels via activation of the NADPH oxidase and increased ROS production. Further, we show that p66^{Shc} expression is increased in PBMs of patients with ischaemic stroke within 6 h from onset of symptoms and that p66^{Shc} gene expression correlates to short-term neurological outcome.

In mice, we recently showed that constitutive genetic deletion of p66^{Shc} reduces early stroke size and neurological deficits following I/R brain injury.[22] However, the mechanisms of this effect and its clinical relevance remained elusive. Furthermore, the use of constitutive

Table I Characteristics of clinical study population

Study population	**Controls $n = 19$**	**Stroke patients $n = 27$**	***P*-value**	
Age (years) mean (range)	71.8 (63-83)	73.9 (52-90)	0.42	
Female, *n* (%)	10 (52.6%)	15 (55.6%)	1.0	
Smoking, *n* (%)	1 (5.3%)	6 (22.2%)	0.22	
Hypertension, *n* (%)	10 (52.6%)	15 (55.6%)	1.0	
Dyslipidaemia, *n* (%)	2 (10.5%)	4 (14.8%)	1.0	
Atrial fibrillation, *n* (%)	0	4 (14.8%)	0.13	
Coronary artery disease, *n* (%)	0	5 (18.5%)	0.07	
Previous stroke/TIA, *n* (%)	0	4 (14.8%)	0.13	
Peripheral artery disease, *n* (%)	0	4 (14.8%)	0.13	
Stroke sub-groups		tPA $n = 14$ (51.9%)	w/o tPA $n = 13$ (48.1%)	*P*-value
Age (years) mean (range)		69.4 (52–80)	78.6 (64–90)	0.03
Female, *n* (%)	15 (55.6%)	6	9	0.25
OXFORD classification				
TACI, *n* (%)	12 (44.4%)	4	8	0.12
PACI, *n* (%)	10 (37.0%)	7	3	0.24
LACI, *n* (%)	5 (18.5%)	3	2	1.0
POCI, *n* (%)	0	0	0	
TOAST classification				
Large vessels atherosclerosis, *n* (%)	5 (18.5%)	2	3	0.65
Card ioembolism, *n* (%)	13 (48.1%)	6	7	0.71
Small vessels disease, *n* (%)	1 (3.7%)	1	0	1.0
Undetermined cause, *n* (%)	5 (18.5%)	3	2	1.0
Other cause, *n* (%)	3 (11.1%)	2	1	1.0
Stroke severity assessment				
Admission NIHSS, mean (SD)	13.3 (6.7)	12.1 (5.0)	14.5 (8.1)	0.38
Discharge NIHSS, mean (SD)	10.1 (9.9)	5.8 (5.3)	14.8 (11.9)	0.046
Early complications				
Haemorrhagic transformation, *n* (%)[a]	4 (17.4%)	3	1	0.61
Cerebral oedema, *n* (%)[a]	6 (26.1%)	1	5	0.05

Clinical characteristics of controls and stroke patients do not differ statistically. Sub-group analysis shows statistically significant differences in age and NIHSS at discharge between patients treated with thrombolysis and patients which did not receive thrombolysis. Age is given as mean (with ranges) and NIHSS is expressed as mean ± SD.
TIA, transient ischaemic attack; tPA, tissue plasminogen activator; TACI, total anterior circulation infarct; PACI, partial anterior circulation infarct; LACI, lacunar infarct; POCI, posterior circulation infarct; TOAST, Trial of ORG 10172 in Acute Stroke Treatment; NIHSS, National Institutes of Health Stroke Scale.
[a]Haemorrhagic transformation and cerebral oedema were determined in stroke patients ($n = 23$; tPA $n = 13$, w/otPA $n = 10$) on CT scan at 24 h after initial stroke symptoms.

knockout animals only serves as a proof-of-principle and does not allow delineation of therapeutic time windows as required in the clinical setting. In contrast, RNA interference (RNAi)-based strategies allow to modify the expression of a certain target at the post-transcriptional level, thus making it therapeutically interesting.[42] Indeed, several RNAi-based strategies are under investigation in clinical trials.[43] Here, we used a clinically relevant experimental setup with siRNA delivery upon reperfusion to reduce p66^{Shc} levels. Reperfusion of an occluded vessel allows reoxygenation of the ischaemic area which promotes recovery of penumbral areas.[44] Nevertheless paradoxically, re-introduction of oxygen in a previously ischaemic area also causes a surge in free radical generation[11] which interferes with the recovery processes. Indeed, we demonstrate here that silencing of the pro-oxidant p66^{Shc} after the ischaemic episode and upon reperfusion, as it would be the case in stroke patients presenting at the emergency room undergoing thrombolytic treatment, reduces lesion volume, improves neurological function, and increases survival. These data highlight the potential of p66^{Shc} as novel therapeutic target in stroke patients undergoing thrombolysis.

Given the key role of BBB permeability in determining stroke outcome,[6] we characterized its integrity by analysing Evans blue extravasation, a known indicator for vascular leakage.[9,30,31,45] Indeed, and in line with the improved stroke outcome in the sip66^{Shc} stroke mice, BBB disruption was blunted after p66^{Shc} silencing compared with control mice. Cerebral microvascular endothelial cells connected via tight and adherens junctional proteins make up the BBB.[7] A disruption of this tightly regulated structure is known to occur in I/R brain injury and is responsible for vascular leakage and in turn oedema formation.[9–11] To investigate the molecular mechanisms by which p66^{Shc} preserves BBB integrity after I/R brain injury, we focused *in vivo* as well as *in vitro* on claudin-5, occludin and VE-cadherin, three major junctional proteins.[7] Consistently, we

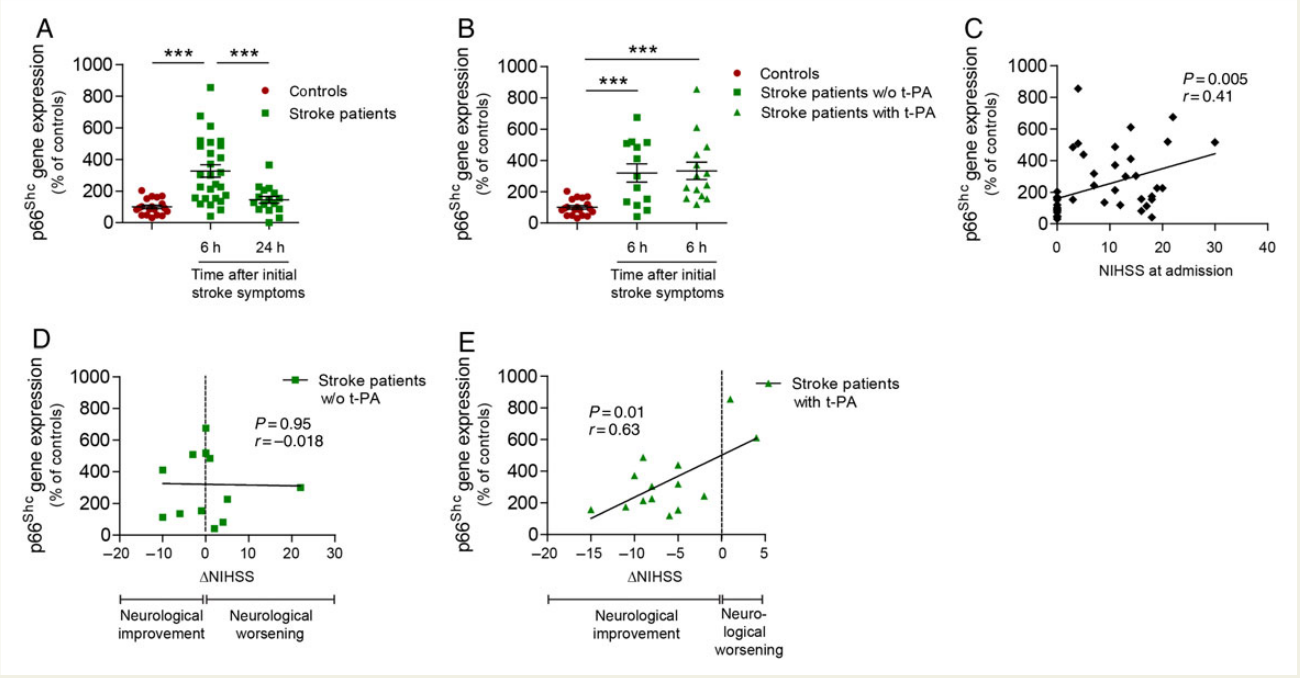

Figure 6 p66^{Shc} gene expression in PBMs of ischaemic stroke patients. (*A*) Real-time polymerase chain reaction determined increased p66^{Shc} mRNA levels in stroke patients 6 h ($n = 27$), but not 24 h ($n = 16$) after initial stroke symptoms compared with the levels of control subjects ($n = 19$). Data are expressed as mean ± s.e.m. (*B*) p66^{Shc} gene expression 6 h after initial stroke symptoms was determined in sub-groups of stroke patients according as they did (t-PA), or did not (w/o t-PA) receive thrombolytic treatment. Values from controls are also shown for comparisons. p66^{Shc} mRNA levels are not different between both stroke sub-groups (w/o t-PA: $n = 13$; t-PA: $n = 14$). Both sub-groups show higher p66^{Shc} levels compared with controls. Data are expressed as mean ± s.e.m. (*C*) Correlation between p66^{Shc} gene expression and NIHSS at admission of all study subjects ($n = 46$). (*D* and *E*) Correlation analysis of p66^{Shc} transcripts and delta NIHSS (NIHSS discharge − NIHSS admission) in w/o t-PA patients ($n = 13$) and in t-PA patients ($n = 14$). For (*C*–*E*) linear regression trend lines are illustrated. ***$P < 0.001$. NIHSS, National Institutes of Health Stroke Scale; t-PA, tissue plasminogen activator.

found less reduction in claudin-5 levels after silencing of p66^{Shc}. In contrast, occludin and VE-cadherin levels remained unaltered in both experimental settings. Our data obtained on murine as well as primary human cells indicate that p66^{Shc} mediates BBB disruption by acting specifically on claudin-5 rather than occludin and VE-cadherin.

To characterize the molecular regulation of claudin-5 by p66^{Shc}, we exposed primary HBMECs to H/R, to mimic *in vivo* settings. Exposure of HBMECs to H/R, but not to hypoxia, increased phosphorylation of p66^{Shc} at Ser36 confirming previous data in renal tubular epithelial cells.[46] Together with our *in vivo* data, these results suggest that p66^{Shc} is mainly involved in mediating its deleterious effects during reperfusion, rather than during ischaemia. Endothelial ROS production and NO bioavailability are both critical for I/R-induced alteration in BBB permeability and stroke outcome[12,47] and ROS are known to influence claudin-5 levels in brain endothelial cells.[48] Here, we demonstrate *in vitro* evidence that endothelial p66^{Shc} silencing in H/R preserves NO bioavailability, reduces NADPH oxidase activation, and decreases ROS generation thus blunting the reduction in claudin-5 levels. This pathway may be also relevant *in vivo*.

To study p66^{Shc} gene regulation in stroke patients, we performed proof-of-principle experiments assessing its expression in PBMs of acute ischaemic stroke patients. Although it would be of particular interest and relevance to elucidate the role of cerebrovascular p66^{Shc} in stroke patients, sample collection in humans would prove extremely difficult thus, we selected PBMs since those are easily obtainable from whole blood and could still give us interesting insights into gene expression changes. Here we found that p66^{Shc} mRNA levels were increased 6 h after initial stroke symptoms and then returned to basal levels at 24 h. Moreover, p66^{Shc} expression at 6 h correlated to short-term neurological outcome (delta NIHSS) in stroke patients. Interestingly, delta NIHSS correlated to p66^{Shc} expression only in patients undergoing thrombolysis, but not in those without. Although thrombolysis is known to improve neurological outcome after stroke,[5] it is also associated with early reperfusion-induced BBB damage[49] which is known to be mediated by ROS and affects stroke outcome.[6] An increased vascular leakage also favours the accumulation of blood circulating cells in brain tissue thus causing tissue damage via production of free radicals.[11,50] This could explain why the correlation between neurological outcome and p66^{Shc} expression is found only in thrombolytic patients where monocytic p66^{Shc}-induced ROS production and the consequent damage is likely more pronounced. In contrast, in patients not undergoing thrombolysis, the role of reperfusion-induced ROS-dependent injury is less prominent and thus neurological damage is less likely to be dependent on p66^{Shc}-mediated ROS.

In summary, the present study sets the stage for follow-up clinical studies aimed at assessing the potential for p66^{Shc} to become a novel therapeutic target as an adjunct of thrombolysis for the management of acute ischaemic stroke.

Supplementary material

Supplementary Material is available at *European Heart Journal* online.

Acknowledgements

We thank Prof. Gianvito Martino from the Neuroimmunology Unit, Division of Neuroscience, Institute of Experimental Neurology, San Raffaele Scientific Institute Milan, Italy, for his intellectual and technical contribution.

Funding

This work was supported by the Swiss National Science Foundation (grant number 310030_147017 to G.G.C., 310030-135815 to T.F.L., and 136822 to J.K.) and Helmut-Horten Foundation to G.G.C.

Conflict of interest: none declared.

References

1. Nichols M, Townsend N, Scarborough P, Rayner M. Cardiovascular disease in Europe 2014: epidemiological update. *Eur Heart J* 2014;**35**:2950–2959.
2. O'Collins VE, Macleod MR, Donnan GA, Horky LL, van der Worp BH, Howells DW. 1,026 experimental treatments in acute stroke. *Ann Neurol* 2006;**59**:467–477.
3. Fisher M, Feuerstein G, Howells DW, Hurn PD, Kent TA, Savitz SI, Lo EH, Group S. Update of the stroke therapy academic industry roundtable preclinical recommendations. *Stroke* 2009;**40**:2244–2250.
4. Spescha RD, Sessa M, Camici GG. Angiopoietin-like 4 and ischaemic stroke: a promising start. *Eur Heart J* 2013;**34**:3603–3605.
5. Tissue plasminogen activator for acute ischemic stroke. The national institute of neurological disorders and stroke RT-PA stroke study group. *N Engl J Med* 1995;**333**:1581–1587.
6. Obermeier B, Daneman R, Ransohoff RM. Development, maintenance and disruption of the blood-brain barrier. *Nat Med* 2013;**19**:1584–1596.
7. Zlokovic BV. The blood-brain barrier in health and chronic neurodegenerative disorders. *Neuron* 2008;**57**:178–201.
8. Iadecola C, Anrather J. The immunology of stroke: from mechanisms to translation. *Nat Med* 2011;**17**:796–808.
9. Su EJ, Fredriksson L, Geyer M, Folestad E, Cale J, Andrae J, Gao Y, Pietras K, Mann K, Yepes M, Strickland DK, Betsholtz C, Eriksson U, Lawrence DA. Activation of PDGF-CC by tissue plasminogen activator impairs blood-brain barrier integrity during ischemic stroke. *Nat Med* 2008;**14**:731–737.
10. Lo EH, Dalkara T, Moskowitz MA. Mechanisms, challenges and opportunities in stroke. *Nat Rev Neurosci* 2003;**4**:399–415.
11. Rodrigues SF, Granger DN. Role of blood cells in ischaemia-reperfusion induced endothelial barrier failure. *Cardiovasc Res* 2010;**87**:291–299.
12. Moskowitz MA, Lo EH, Iadecola C. The science of stroke: mechanisms in search of treatments. *Neuron* 2010;**67**:181–198.
13. Pelicci G, Lanfrancone L, Grignani F, McGlade J, Cavallo F, Forni G, Nicoletti I, Grignani F, Pawson T, Pelicci PG. A novel transforming protein (SHC) with an SH2 domain is implicated in mitogenic signal transduction. *Cell* 1992;**70**:93–104.
14. Migliaccio E, Mele S, Salcini AE, Pelicci G, Lai KM, Superti-Furga G, Pawson T, Di Fiore PP, Lanfrancone L, Pelicci PG. Opposite effects of the p52shc/p46shc and p66shc splicing isoforms on the EGF receptor-MAP kinase-fos signalling pathway. *EMBO J* 1997;**16**:706–716.
15. Camici GG, Schiavoni M, Francia P, Bachschmid M, Martin-Padura I, Hersberger M, Tanner FC, Pelicci P, Volpe M, Anversa P, Luscher TF, Cosentino F. Genetic deletion of p66(Shc) adaptor protein prevents hyperglycemia-induced endothelial dysfunction and oxidative stress. *Proc Natl Acad Sci USA* 2007;**104**:5217–5222.
16. Francia P, delli Gatti C, Bachschmid M, Martin-Padura I, Savoia C, Migliaccio E, Pelicci PG, Schiavoni M, Luscher TF, Volpe M, Cosentino F. Deletion of p66shc gene protects against age-related endothelial dysfunction. *Circulation* 2004;**110**:2889–2895.
17. Napoli C, Martin-Padura I, de Nigris F, Giorgio M, Mansueto G, Somma P, Condorelli M, Sica G, De Rosa G, Pelicci P. Deletion of the p66Shc longevity gene reduces systemic and tissue oxidative stress, vascular cell apoptosis, and early atherogenesis in mice fed a high-fat diet. *Proc Natl Acad Sci USA* 2003;**100**:2112–2116.
18. Zaccagnini G, Martelli F, Fasanaro P, Magenta A, Gaetano C, Di Carlo A, Biglioli P, Giorgio M, Martin-Padura I, Pelicci PG, Capogrossi MC. p66ShcA modulates tissue response to hindlimb ischemia. *Circulation* 2004;**109**:2917–2923.
19. Francia P, Cosentino F, Schiavoni M, Huang Y, Perna E, Camici GG, Luscher TF, Volpe M. p66(Shc) protein, oxidative stress, and cardiovascular complications of diabetes: the missing link. *J Mol Med* 2009;**87**:885–891.
20. Camici GG, Shi Y, Cosentino F, Francia P, Luscher TF. Anti-aging medicine: molecular basis for endothelial cell-targeted strategies – a mini-review. *Gerontology* 2011;**57**:101–108.
21. Cosentino F, Francia P, Camici GG, Pelicci PG, Luscher TF, Volpe M. Final common molecular pathways of aging and cardiovascular disease: role of the p66Shc protein. *Arterioscler Thromb Vasc Biol* 2008;**28**:622–628.
22. Spescha RD, Shi Y, Wegener S, Keller S, Weber B, Wyss MM, Lauinger N, Tabatabai G, Paneni F, Cosentino F, Hock C, Weller M, Nitsch RM, Luscher TF, Camici GG. Deletion of the ageing gene p66(Shc) reduces early stroke size following ischaemia/reperfusion brain injury. *Eur Heart J* 2013;**34**:96–103.
23. Pagnin E, Fadini G, de Toni R, Tiengo A, Calo L, Avogaro A. Diabetes induces p66shc gene expression in human peripheral blood mononuclear cells: relationship to oxidative stress. *J Clin Endocrinol Metab* 2005;**90**:1130–1136.
24. Bamford J, Sandercock P, Dennis M, Burn J, Warlow C. Classification and natural history of clinically identifiable subtypes of cerebral infarction. *Lancet* 1991;**337**:1521–1526.
25. Adams HP Jr, Bendixen BH, Kappelle LJ, Biller J, Love BB, Gordon DL, Marsh EE 3rd. Classification of subtype of acute ischemic stroke. Definitions for use in a multicenter clinical trial. TOAST. Trial of Org 10172 in Acute Stroke Treatment. *Stroke* 1993;**24**:35–41.
26. Franzeck FC, Hof D, Spescha RD, Hasun M, Akhmedov A, Steffel J, Shi Y, Cosentino F, Tanner FC, von Eckardstein A, Maier W, Luscher TF, Wyss CA, Camici GG. Expression of the aging gene p66Shc is increased in peripheral blood monocytes of patients with acute coronary syndrome but not with stable coronary artery disease. *Atherosclerosis* 2012;**220**:282–286.
27. Paneni F, Mocharla P, Akhmedov A, Costantino S, Osto E, Volpe M, Luscher TF, Cosentino F. Gene silencing of the mitochondrial adaptor p66(Shc) suppresses vascular hyperglycemic memory in diabetes. *Circ Res* 2012;**111**:278–289.
28. Swanson RA, Morton MT, Tsao-Wu G, Savalos RA, Davidson C, Sharp FR. A semiautomated method for measuring brain infarct volume. *J Cereb Blood Flow Metab* 1990;**10**:290–293.
29. Bederson JB, Pitts LH, Tsuji M, Nishimura MC, Davis RL, Bartkowski H. Rat middle cerebral artery occlusion: evaluation of the model and development of a neurologic examination. *Stroke* 1986;**17**:472–476.
30. Gursoy-Ozdemir Y, Bolay H, Saribas O, Dalkara T. Role of endothelial nitric oxide generation and peroxynitrite formation in reperfusion injury after focal cerebral ischemia. *Stroke* 2000;**31**:1974–1980; discussion 1981.
31. Bouleti C, Mathivet T, Coqueran B, Serfaty JM, Lesage M, Berland E, Ardidie-Robouant C, Kauffenstein G, Henrion D, Lapergue B, Mazighi M, Duyckaerts C, Thurston G, Valenzuela DM, Murphy AJ, Yancopoulos GD, Monnot C, Margaill I, Germain S. Protective effects of angiopoietin-like 4 on cerebrovascular and functional damages in ischaemic stroke. *Eur Heart J* 2013;**34**:3657–3668.
32. Spescha RD, Glanzmann M, Simic B, Witassek F, Keller S, Akhmedov A, Tanner FC, Luscher TF, Camici GG. Adaptor protein p66Shc mediates hypertension-associated, cyclic stretch-dependent, endothelial damage. *Hypertension* 2014;**64**:347–353.
33. Besler C, Heinrich K, Rohrer L, Doerries C, Riwanto M, Shih DM, Chroni A, Yonekawa K, Stein S, Schaefer N, Mueller M, Akhmedov A, Daniil G, Manes C, Templin C, Wyss C, Maier W, Tanner FC, Matter CM, Corti R, Furlong C, Lusis AJ, von Eckardstein A, Fogelman AM, Luscher TF, Landmesser U. Mechanisms underlying adverse effects of HDL on eNOS-activating pathways in patients with coronary artery disease. *J Clin Invest* 2011;**121**:2693–2708.
34. Shi Y, Cosentino F, Camici GG, Akhmedov A, Vanhoutte PM, Tanner FC, Luscher TF. Oxidized low-density lipoprotein activates p66Shc via lectin-like oxidized low-density lipoprotein receptor-1, protein kinase C-beta, and c-Jun N-terminal kinase kinase in human endothelial cells. *Arterioscler Thromb Vasc Biol* 2011;**31**:2090–2097.
35. Cecchelli R, Berezowski V, Lundquist S, Culot M, Renftel M, Dehouck MP, Fenart L. Modelling of the blood-brain barrier in drug discovery and development. *Nat Rev Drug Discov* 2007;**6**:650–661.
36. Walchli T, Pernet V, Weinmann O, Shiu JY, Guzik-Kornacka A, Decrey G, Yuksel D, Schneider H, Vogel J, Ingber DE, Vogel V, Frei K, Schwab ME. Nogo-A is a negative regulator of CNS angiogenesis. *Proc Natl Acad Sci USA* 2013;**110**:E1943–E1952.
37. Migliaccio E, Giorgio M, Mele S, Pelicci G, Reboldi P, Pandolfi PP, Lanfrancone L, Pelicci PG. The p66shc adaptor protein controls oxidative stress response and life span in mammals. *Nature* 1999;**402**:309–313.

38. Drummond GR, Selemidis S, Griendling KK, Sobey CG. Combating oxidative stress in vascular disease: NADPH oxidases as therapeutic targets. *Nat Rev Drug Discov* 2011;**10**:453–471.
39. Tomilov AA, Bicocca V, Schoenfeld RA, Giorgio M, Migliaccio E, Ramsey JJ, Hagopian K, Pelicci PG, Cortopassi GA. Decreased superoxide production in macrophages of long-lived p66Shc knock-out mice. *J Biol Chem* 2010;**285**:1153–1165.
40. Zehendner CM, Librizzi L, Hedrich J, Bauer NM, Angamo EA, de Curtis M, Luhmann HJ. Moderate hypoxia followed by reoxygenation results in blood-brain barrier breakdown via oxidative stress-dependent tight-junction protein disruption. *PLoS ONE* 2013;**8**:e82823.
41. Heumuller S, Wind S, Barbosa-Sicard E, Schmidt HH, Busse R, Schroder K, Brandes RP. Apocynin is not an inhibitor of vascular NADPH oxidases but an antioxidant. *Hypertension* 2008;**51**:211–217.
42. Mello CC, Conte D Jr. Revealing the world of RNA interference. *Nature* 2004;**431**:338–342.
43. Kanasty R, Dorkin JR, Vegas A, Anderson D. Delivery materials for siRNA therapeutics. *Nat Mater* 2013;**12**:967–977.
44. Astrup J, Symon L, Branston NM, Lassen NA. Cortical evoked potential and extracellular K+ and H+ at critical levels of brain ischemia. *Stroke* 1977;**8**:51–57.
45. Yepes M, Sandkvist M, Moore EG, Bugge TH, Strickland DK, Lawrence DA. Tissue-type plasminogen activator induces opening of the blood-brain barrier via the LDL receptor-related protein. *J Clin Invest* 2003;**112**:1533–1540.
46. Zhao WY, Han S, Zhang L, Zhu YH, Wang LM, Zeng L. Mitochondria-targeted antioxidant peptide SS31 prevents hypoxia/reoxygenation-induced apoptosis by down-regulating p66Shc in renal tubular epithelial cells. *Cell Physiol Biochem* 2013;**32**:591–600.
47. Dalkara T, Yoshida T, Irikura K, Moskowitz MA. Dual role of nitric oxide in focal cerebral ischemia. *Neuropharmacology* 1994;**33**:1447–1452.
48. Schreibelt G, Kooij G, Reijerkerk A, van Doorn R, Gringhuis SI, van der Pol S, Weksler BB, Romero IA, Couraud PO, Piontek J, Blasig IE, Dijkstra CD, Ronken E, de Vries HE. Reactive oxygen species alter brain endothelial tight junction dynamics via RhoA, PI3 kinase, and PKB signaling. *FASEB J* 2007;**21**:3666–3676.
49. Kastrup A, Groschel K, Ringer TM, Redecker C, Cordesmeyer R, Witte OW, Terborg C. Early disruption of the blood-brain barrier after thrombolytic therapy predicts hemorrhage in patients with acute stroke. *Stroke* 2008;**39**:2385–2387.
50. Kochanek PM, Hallenbeck JM. Polymorphonuclear leukocytes and monocytes/macrophages in the pathogenesis of cerebral ischemia and stroke. *Stroke* 1992;**23**:1367–1379.

Supplemental Material

Post-Ischemic Silencing of p66^{Shc} Reduces Ischaemia/Reperfusion Brain Injury and its Expression Correlates to Clinical Outcome in Stroke

Spescha RD[1,2], Klohs J[3], Semerano A[4], Giacalone G[4], Derungs RS[5], Reiner MF[1,2], Rodriguez Gutierrez D[1], Mendez-Carmona N[1], Glanzmann M[1,2], Savarese G[1,2], Kränkel N[1,2,9], Akhmedov A[1,2], Keller S[1,2], Mocharla P[1,2], Kaufmann MR[2,6], Wenger RH[2,6], Vogel J[7], Kulic L[5], Nitsch RM[5], Beer JH[10], Peruzzotti-Jametti L[4], Sessa M[4], Lüscher TF[1,2,8], Camici GG[1,2]

Methods

In vivo p66^{Shc} silencing

In vivo p66^{Shc} silencing was performed as described[1]. Briefly, predesigned siRNA targeting p66^{Shc} (sense: 5'-UGAGUCUCUGUCAUCGCUG[dT][dT]-3'; antisense: 5'-CAGCGAUGACAGAGACUCA[dT][dT]-3' (Microsynth) were injected intravenously randomized. As a negative control, a scrambled siRNA was used (sense: 5'-UACACACUCUCGUCUCU[dT][dT]-3'; antisense: 5'-AGAGACGAGAGUGUGUA[dT][dT]-3') (Microsynth). 1.6 nmol of siRNA were incubated with a mixture of 150 mmol/L NaCl solution–jetPEI® (Polyplus Transfection™) delivery reagent for 15 min before injecting into the tail vein of the mouse. To localise the distribution of sip66^{Shc} in cerebral arteries, wt mice were injected with fluorescence dye-labelled p66^{Shc} siRNA (Alexa546-sip66^{Shc}, Qiagen), as previously reported[1]. 1.6 nmol of Alexa546-sip66^{Shc} were incubated with a mixture of 150 mmol/L NaCl solution–jetPEI® (Polyplus Transfection™) delivery reagent for 15 min before injecting into the tail vein of the mouse. 24 h after Alexa546-sip66^{Shc} injection, the brain was removed, cut into ~1 mm³ large pieces and digested under constant movement by collagenase I (0.2%; Worthington) and DNAse (0.01%; Worthington) for 30 min at 37°C. Tissue digest was filtered through 100 µm cell strainers to obtain single cell solutions. Cells were stained with anti-mouse CD45-APC and anti-

mouse CD31-AlexaFluor 488, fixed and nuclei counterstained with Hoechst 33342. Cell suspensions were acquired on a Fortessa flow cytometer (Becton Dickinson).

Magnetic resonance imaging (MRI)

Lesion development was monitored after MCAO on a Bruker PharmaScan 47/16 (Bruker BioSpin GmbH) operating at 4.7 T and equipped with a volume resonator operating in quadrature mode for excitation and a four element phased array surface coil for signal reception. Anaesthesia was induced using 3% isoflurane (Abbott) in a 4:1 air/oxygen mixture. During MRI acquisition, mice were kept under isoflurane anaesthesia (1.5%). During the scan session body temperature was monitored with a rectal temperature probe (MLT415, ADInstruments) and kept at 36±0.55°C using a warm water circuit integrated into the animal support (Bruker BioSpin GmbH).Tri-pilot scans were used for accurate positioning of the animal head inside the magnet. For diffusion-weighted imaging (DWI) a four-shot spin echo-echo planar imaging (SE-EPI) sequence with TE/TR =29.4/3000 ms was used, starting with 4 dummy scans. Twelve 1-mm thick slices with an interslice distance of 1.3 mm were acquired with a FOV of 3.3 cm x 2 cm and a matrix size of 128 x 128, resulting in a nominal voxel size of 257 µm x 156 µm. Diffusion-encoding was applied in x-, y- and z-direction (gradient pulse duration = 7 ms, gradient pulse separation = 14 ms) with b-values of 100, 200, 400, 600, 800, and 1000 s/mm^2, respectively. The total acquisition time was 3 min 48 s. A T2-weighted spin-echo sequence (TurboRARE) was used with TE/TR= 85/3180 ms, RARE factor = 8 with four averages. Twelve 1-mm thick slices with an interslice distance of 1.3 mm were imaged with a FOV of 2 cm x 2 cm and a matrix size of 200 x 200, resulting in a nominal voxel size of 100 µm x 100 µm. The total acquisition time was 5 min and 18 s. MRI recordings were done in a blinded way by an independent person.

The lesion was determined on maps of the apparent diffusion coefficient (ADC) derived from diffusion-weighted images as areas of significant reduction of the ADC compared to the unaffected, contralateral side. The lesion in the T2-weighted image was determined as hyperintense areas compared to the contralateral hemisphere. Lesion volumes were quantified blinded by drawing region of interests around the areas of reduced ADC and hyperintensities in T2-weighted images in five MRI slices using a ROI tool (Paravision,

Bruker). Brain infarct volumes were calculated by summing the volumes of each section and correcting for brain swelling, as described[2].

Evans blue extravasation

Determination of BBB permeability after MCAO was done by evaluating Evans blue extravasation, as described[3]. Briefly, 0.15 ml of 5% Evans blue (Sigma) was injected into the tail vein of each mouse 1 h before culling. Following transcardial perfusion with saline, ipsilateral brain hemisphere was homogenised in 0.1 mol/L PBS and centrifuged at 1000 rcf for 15 min. The resulting supernatant was incubated for 18 h at 4°C in 100% trichloroacetic acid. Following centrifugation at 1000 rcf for 30 min, Evans blue absorbance in the supernatant was measured spectrophotometrically at 610 nm wavelength and Evans blue concentration was calculated from standard solutions.

Immunofluorescence staining

Frozen brains were cut into 6 µm thick slices on a cryostat (Leica Cm 1900). Immunofluorescent analysis was performed as described[4]. Briefly, following fixation in 4% paraformaldehyde for 1 h at room temperature (RT), brain slices were washed in TBS-T (0.1 mol/L Tris-HCl, 150 mmol/L NaCl, 0.2% Triton X-100, pH 7.4), blocked for 2 h at RT in TBS-T containing 5% donkey serum, and incubated with primary antibodies. Anti-claudin-5 (Invitrogen), anti-VE-cadherin (Millipore), and anti-occludin (BD Transduction Laboratories™) antibodies were diluted 1:100 in TBS-T containing 2.5% donkey serum. The biotin-XX isolectin GS-IB_4 conjugate (Life Technologies™) was used at 1:200 dilution. Secondary antibody Cy3-AffiniPure F(ab')2 Fragment Donkey Anti-Mouse IgG (H+L) (Jackson ImmunoResearch) and Cy2-Streptavidin (Jackson ImmunoResearch) were used at 1:400 dilution. Brain slices were mounted on slides in hydromount mounting medium (national diagnostics) and images were taken using a Leica Dm4000 B microscope. Stained area of claudin-5, VE-cadherin, or occludin was measured using ImageJ Software and normalised to the total endothelial cell surface (assessed by isolectin B_4 staining).

Quantitative real-time PCR

Determination of $p66^{Shc}$ gene expression was done as previously described[5]. TaqMan® Gene Expression Assays (Applied Biosystems™) was used for real-time PCR and performed on a 7500 Fast Real-Time PCR System (Applied Biosystems™). Each reaction included 2 µl of cDNA, 1 µl of specific TaqMan® MGB probes and primers for human $p66^{Shc}$ or mouse $p66^{Shc}$ (predesigned by Applied Biosystems™), 10 µl of TaqMan® Universal PCR Master Mix (Applied Biosystems™), and 7 µl of H_2O (total 20 µl). TATA box binding protein (TBP) (Applied Biosystems™), or ribosomal 18S RNA (Applied Biosystems™) was used as an endogenous control. For quantification, the $2^{-\Delta Ct}$ method was used. $p66^{Shc}$ transcript levels in PBM of ischaemic stroke patients were expressed as percentage of controls. $p66^{Shc}$ transcript levels in MCA of $sip66^{Shc}$ mice were expressed as percentage of siScr mice.

siRNA transfection in HBMEC

siRNA transfection in HBMEC was done as described[6]. HBMEC were incubated with predesigned siRNA targeting $p66^{Shc}$ (sense: 5′-AUGAGUCUCUGUCAUCGCU[dT][dT]-3′; antisense: 5'-AGCGAUGACAGAGACUCAU[dT][dT]-3') (Sigma-Aldrich) for 4 h in serum-free and antibiotics-free EBM-2 medium (Lonza) at final concentration of 25 nmol/L using Lipofectamine®RNAiMAX Reagent (Invitrogen), followed by incubation in normal growth medium for another 20 h. Scrambled siRNA (sense: 5'-GAUCAUACGUGCGAUCAGA[dT][dT]-3'; antisense: 5'-UCUGAUCGCACGUAUGAUC[dT][dT]-3'; 25 nmol/L) (Sigma-Aldrich) or vehicle alone were used as negative controls.

Immunoblotting

Immunoblot analysis was performed as previously described[6]. For animal experiments, basilar arteries were homogenised and lysed in 50 mmol/L Tris-HCl pH 7.5, 150 mmol/L NaCl, 1 mmol/L EDTA pH 8.0, 1 mmol/L NaF, 1 mmol/L DTT, 10 µg/µl aprotinin, 10 µg/µl leupeptin, 0.1 mmol/L Na_3VO_4, 1 mmol/L PMSF, and 0.5% NP-40. For cell culture experiments, cells were lysed in 50 mmol/L Tris-HCl pH 7.5, 150 mmol/L NaCl, 1 mmol/L EDTA pH 8.0, 1 mmol/L NaF, 1 mmol/L DTT, 10 µg/µl aprotinin, 10 µg/µl leupeptin, 0.1

mmol/L Na_3VO_4, 1 mmol/L PMSF, and 0.5% NP-40. SDS-PAGE was performed for protein separation. Antibodies against anti-SHC (BD Transduction Laboratories™), and anti-Shc/p66 (pSer36) (Calbiochem) were used at 1:1000 and 1:100 dilutions, respectively. Antibodies against p-eNOS (Thr495), p-eNOS (Ser1177), and eNOS (all from BD Transduction Laboratories™) were used at 1:5000, 1:2000 and 1:2000 dilutions, respectively. Both, anti-Claudin-5 (Invitrogen) and anti-human-HIF-1α (BD Transduction Laboratories™) antibodies were used at 1:1000 dilution. Anti-VE-Cadherin (Millipore) and anti-Occludin (BD Transduction Laboratories™) antibodies were diluted at 1:2000 and 1:500 dilutions, respectively. Blots were normalised to glyceraldehyde 3-phosphate dehydrogenase (GAPDH) protein levels (1:20000 dilution; Millipore). Anti-rabbit and anti-mouse secondary antibodies were from SouthernBiotech.

Measurement of O_2^- production

Electron spin resonance (ESR) spectroscopy was applied to measure O_2^- production, as described[6, 7]. O_2^- production was determined on a ESR spectrometer (Bruker) in cells suspended in Krebs-HEPES solution (Noxygen) containing 200 µmol/L 1-hydroxy-3-methoxycarbonyl-2,2,5,5-tetramethylpyrrolidine hydrochloride (Noxygen), 5 µmol/L sodium diethyldithiocarbamate trihydrate (Noxygen), and 25 µmol/L deferoxamine methanesulfonate (Noxygen) and by using following instrumental settings: center field, 3469.0 G; sweep width, 10.00 G; microwave frequency, 9.76 GHz; microwave power, 19.91 mW; modulation frequency, 86.00 kHz; modulation amplitude, 2.60 G; and number of scans, 10. A temperature-controlled system maintained the temperature at 37°C.

Measurement of NO bioavailability

ESR spectroscopy was applied to measure NO bioavailability, as described[1, 6, 8]. After incubation with Krebs-HEPES – $Fe(DETC)_2$ solution for 1 h at 37ºC, cells collected in Krebs-HEPES solution (Noxygen) were snap frozen in liquid nitrogen and measured on an ESR spectrometer (Bruker) using the following instrumental settings: center field, 3455.00 G; sweep width, 80.00 G microwave frequency, 9.78 GHz; microwave power, 39.72 mW; modulation frequency, 86.00 kHz; modulation amplitude, 10.34 G; and number of scans, 10.

References

1. Paneni F, Mocharla P, Akhmedov A, Costantino S, Osto E, Volpe M, Luscher TF, Cosentino F. Gene silencing of the mitochondrial adaptor p66(Shc) suppresses vascular hyperglycemic memory in diabetes. *Circ Res* 2012;**111**(3):278-289.
2. Swanson RA, Morton MT, Tsao-Wu G, Savalos RA, Davidson C, Sharp FR. A semiautomated method for measuring brain infarct volume. *J Cereb Blood Flow Metab* 1990;**10**(2):290-293.
3. Gursoy-Ozdemir Y, Bolay H, Saribas O, Dalkara T. Role of endothelial nitric oxide generation and peroxynitrite formation in reperfusion injury after focal cerebral ischemia. *Stroke* 2000;**31**(8):1974-1980; discussion 1981.
4. Bouleti C, Mathivet T, Coqueran B, Serfaty JM, Lesage M, Berland E, Ardidie-Robouant C, Kauffenstein G, Henrion D, Lapergue B, Mazighi M, Duyckaerts C, Thurston G, Valenzuela DM, Murphy AJ, Yancopoulos GD, Monnot C, Margaill I, Germain S. Protective effects of angiopoietin-like 4 on cerebrovascular and functional damages in ischaemic stroke. *Eur Heart J* 2013;**34**(47):3657-3668.
5. Franzeck FC, Hof D, Spescha RD, Hasun M, Akhmedov A, Steffel J, Shi Y, Cosentino F, Tanner FC, von Eckardstein A, Maier W, Luscher TF, Wyss CA, Camici GG. Expression of the aging gene p66Shc is increased in peripheral blood monocytes of patients with acute coronary syndrome but not with stable coronary artery disease. *Atherosclerosis* 2012;**220**(1):282-286.
6. Spescha RD, Glanzmann M, Simic B, Witassek F, Keller S, Akhmedov A, Tanner FC, Luscher TF, Camici GG. Adaptor Protein p66Shc Mediates Hypertension-Associated, Cyclic Stretch-Dependent, Endothelial Damage. *Hypertension* 2014;**64**(2):347-353.
7. Shi Y, Cosentino F, Camici GG, Akhmedov A, Vanhoutte PM, Tanner FC, Luscher TF. Oxidized low-density lipoprotein activates p66Shc via lectin-like oxidized low-density lipoprotein receptor-1, protein kinase C-beta, and c-Jun N-terminal kinase kinase in human endothelial cells. *Arterioscler Thromb Vasc Biol* 2011;**31**(9):2090-2097.
8. Besler C, Heinrich K, Rohrer L, Doerries C, Riwanto M, Shih DM, Chroni A, Yonekawa K, Stein S, Schaefer N, Mueller M, Akhmedov A, Daniil G, Manes C, Templin C, Wyss C, Maier W, Tanner FC,

Matter CM, Corti R, Furlong C, Lusis AJ, von Eckardstein A, Fogelman AM, Luscher TF, Landmesser U. Mechanisms underlying adverse effects of HDL on eNOS-activating pathways in patients with coronary artery disease. *J Clin Invest* 2011;**121**(7):2693-2708.

.